# EMISSION AND CONTROL OF $H^+$ IONS NEAR AN ELECTRON-PHOTON CONVERSION TARGET

A. Compant La Fontaine, D. Guilhem, J.L. Lemaire, C. Quine, Département de Physique Théorique et Appliquée, CEA/DAM Ile-de-France, BP12–F 91680, Bruyères-le-Châtel, France

*Abstract*

During the beam pulse of a high-intensity relativistic electron beam focused on a tantalum target for X-ray production, a large amount of ions is expected to be produced and subsequently to degrade the radiographic source spot size [1,2]. The emission of $H^+$ ions has been observed in the last experiments thanks to a time-of-flight diagnostic [3]. An improved ion emission model, taking into account the desorption of H atoms absorbed in the bulk of the target, has been coupled to a Maxwell-Vlasov PIC code [4]. Dynamics of ions and $H^+$ current which reach the time-of-flight diagnostic foil are calculated with this model and compared to the experimental results. It is shown that i) the mean velocity of the ions is in agreement with the experimental results, ii) the ion current is close to the Child-Langmuir theoretical current limit.

We also report on the new self-biased target converter designed to counteract the ionic motion. Successful tests and beam size control along the pulse have been achieved as predicted.

## 1 INTRODUCTION

A high-intensity relativistic electron beam is focused on a tantalum target that converts the electrons into photons via the bremsstrahlung process. The X-ray emission, directed along the beam axis, is used for radiographic purposes. The energy deposited by the beam focused on a small spot size, causes local vaporisation of the target and production of ions. A beam charge neutralisation then occurs, cancelling the average radial electrical field. Therefore, the beam pinches due to the remaining azimuthal magnetic field. The ions are subsequently accelerated downstream in the strong axial electric field induced by the electron beam. Thus, the displacement of the waist from the target along with the ions leads to an increase during the pulse duration of the spot size at the target and would result in a degradation of the sharpness of the radiographic image [1,4]. The ions have been identified on the PIVAIR accelerator facility using a time-of flight diagnostic located 2.5 cm upstream of the target [3].

It turned out that $H^+$ ions mainly contribute to the effect of spot size increase. In order to improve the model of ion emission developed earlier, the hydrogen content in the target was measured by means of the argon-carrier-fusion thermal conductivity method. Atomic ratios for tantalum and gold targets were found to be equal to $H/Ta = 1.9 \times 10^{-3}$ and $H/Au = 1.2 \times 10^{-3}$.

Then, the emission model VAPOR already dealing with the production of $H^+$ ions from the bulk of the target [4] has been extended to the dissociation of mono-layers of water adsorbed at the target surface.

## 2 EMISSION MODEL

The energy density deposited on the target surface induces a fast local raise up of the target temperature. In the VAPOR model, the temperature raise takes into account the H atoms absorbed in the target bulk and the molecules of water adsorbed at the target surface.

### *2.1 Target Temperature*

The temperature T of the target surface is obtained by integrating step by step the following differential energy equation:

$$dT = \left\{ \frac{I(t)(dE/dx)_0}{\rho e \Delta S} dt - \left( dE_{ions} + dE_{expans} + dL \right) \right\} / a$$

where $(dE / dx)_0$ represents the energy deposited by the electron beam at the target surface by unit of length. The electron-beam is characterized by its current I(t) and surface $\Delta S$. $\rho$ is the specific gravity, e the elementary charge, $E_{ions}$ is the internal energy of the ions, $E_{expans}$ is the energy brought out during the hydrodynamic expansion, L is the fusion enthalpy of the metal. The a denominator term reads as:

$$a = c_{v_M} + \frac{R}{2A_M}\left( \gamma_M w + 3\sum_{z=1} z \frac{n_z}{n} \right) + \sum_{z=1} \zeta_I \frac{A_I}{A_M}\left( c_{v_I} + \frac{R\gamma_I}{2A_I} \right)$$

A is the atomic mass, where the index M and I represent respectively the metal target and the impurity kept in the target (H or $H_2O$). $\zeta_I$ represents the atomic ratio. R is the gas constant, $\gamma = c_p / c_v$, $n_z$ is the density of the ions, z the charge, n is the total atomic density of the metal. $w = \left( \frac{\rho_{vap}}{\rho} \right)^2 \frac{T_{vap}}{T}$, where the vapor density $\rho_{vap}$ and temperature $T_{vap}$ are got by solving the shock-wave equation. The energy loss by blackbody radiation is neglected here.

### *2.1 Desorption of Hydrogen*

The variation of the H concentration $c = n_H/n$ in the bulk metal, at depth x and time t, is obtained by solving the Fick law for an infinite slab, with a boundary condition given by the flux F of atoms ejected from the surface: $F = -D \left. \frac{\partial n}{\partial x} \right|_{x=0}$.

Thus,

$$c_H(x,t) = c_H(x,0) - \frac{2F}{n}\sqrt{\frac{t}{D}}.\mathrm{ierfc}\left(\frac{x}{2\sqrt{Dt}}\right)$$

$D=D_0.\exp(-Ea/T)$ is the diffusion coefficient of H in the metal with the activation energy $E_a$. In addition,

$$F = 2F_{H2} + F_H = \frac{P_{H2}}{\sqrt{2\pi mkT}}\left(\sqrt{2} + \sqrt{\frac{K_e}{P_{H2}}}\right)$$, where $K_e$ is the chemical equilibrium constant of the mixture ($H,H_2$). The H concentration in the metal is related to the the pressure $P_{H2}$ by the Sieverts' law: $c_H = c_0.\sqrt{P_{H2}}.\exp(E_S/T)$.

The concentration $c_H$ and the flux F are easily obtained by solving these equations.

## *2.2 Desorption of Water*

We consider a mono-layer of water adsorbed at the surface of the target. The release of the $H_2O$ molecules from the surface is given, during its heating, by the first order desorption scheme, following Park et al. [5]:

$$\frac{dn}{dt} = k_0 n_S \theta \exp(-E_d/T)$$

where $k_0$ is the preexponential, $n_S$ is the total number of sites available for desorption, θ represents the fraction of occupied sites. The activation energy for desorption $E_d$ is calculated by taking into account the interaction energy of the dimmer $(H_2O)_2$, following Masel [6].

## *2.3 Production of Ions*

As the vapor slab (composed by H, $H_2$ and $H_2O$) expands away from the target, the incident electrons of the beam ionise the H atoms and dissociate the $H_2$ and $H_2O$ molecules. The electrons produced by the ionization (assumed thermalized) also contribute to the ionization of the H atoms, inducing an avalanche effect when the electron density increases. At higher electron density, radiative and three-body recombinations takes place, thus reducing the production of electrons. These effects are considered in the model.

The dissociation of water by thermal process leads to the formation of the following radicals: OH, $H_2$, O, $O_2$ and H , following Lapique et al. [7]. The relative rate coefficients between these radicals are calculated by using the Lapique et al. [7] expressions, assuming that the vapor slab temperature is equal to that of the target. In the vapor slab, the evolution of the $H^+$ density is obtained by solving seven first-order differential coupled equations, including $H^+$, H, $H_2O$, OH, $H_2$, O and $O_2$.

At each time step, the axial ion density profile, the mean density of $H^+$ ions and the associated ionic current $I_{H+}$ are calculated.

At nominal conditions (I= 3 kA, T= 5.8 MeV, Ta target, $r_{RMS}$= 0.45 mm) , it is found by the VAPOR emission model that the Child-Langmuir current (20 A) is reached at about 30 ns. The contribution to the $H^+$ production by one complete monolayer of water at the target surface, together with the H content in the tantalum target (H/Ta= 1.9 $x10^{-3}$) is shown in Fig. 1. The density reaches its maximum at 11 ns for T= 1100 K.

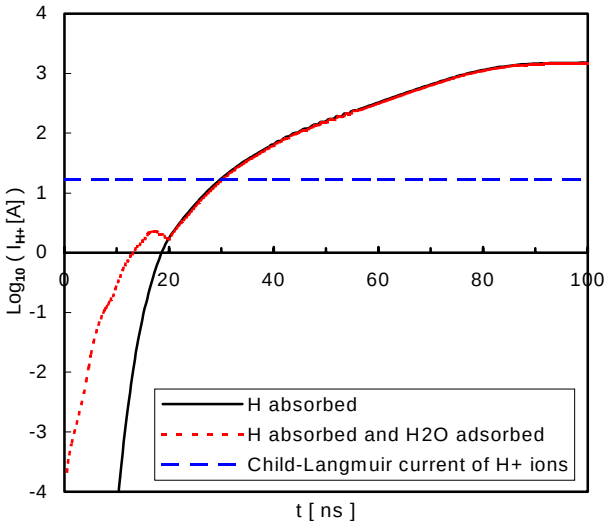


Figure 1: $H^+$ ionic current, calculated by the emission model VAPOR at the tantalum target (H absorbed with H/Ta= 1.9x$10^{-3}$), for two cases: $H_2O$ absent and $H_2O$ present in a mono-layer.

# 3 NUMERICAL SIMULATION

The VAPOR emission model is coupled to the M2V Maxwell-Vlasov PIC code [4] to simulate the experimental results obtained at the PIVAIR facility [3]. The double sheet diagnostic apparatus is located upstream of the target at a distance 2.5 cm. The ions emitted by the target are collected and give the ionic current. The time of flight of the ions was obtained by varying the foil-target distance. $H^+$ ions were identified in this manner.

The time appearance of the ions, the rise time of the ionic current, the plateau current level are the same as calculated and experimentally measured (see Fig. 2).

The ionic current fall-off can be interpreted as the blow-out of the ion beam de-confined under the effect of its own space charge, once the electron beam pulse ended.

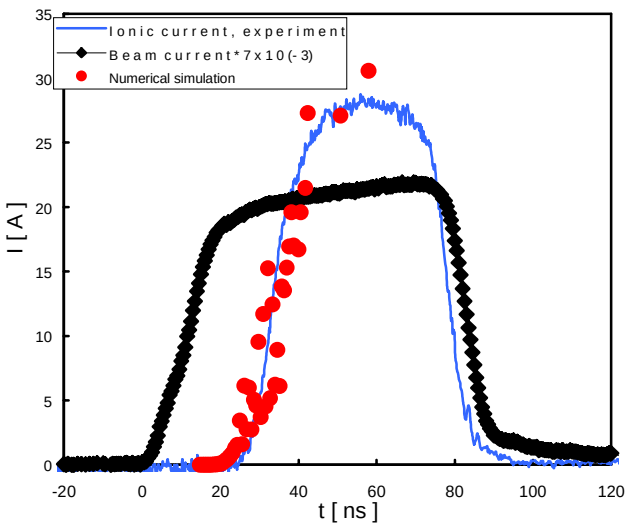


Figure 2: $H^+$ ionic current, experimentally measured [3] and calculated by the coupled VAPOR-M2V model. Experimental conditions : tantalum target, electron beam current 3 kA and 5.8 MeV.

## 4 SELF-BIASED TARGET CONVERTOR

The design of the target chamber was achieved through three steps. At first, numerical simulations were done to optimise the required bias potential. For this study, the particle-in-cell code M2V coupled to an early version of VAPOR was used. Emission of different ion species either at space charge limited current or at lower values was possible. Then the mechanical and electrical designs were pursued, using a finite-element code FLUX 2D to obtain the electric field profile in the target chamber. The equivalent resistor value is made of 4 resistor bars mounted in parallel and supporting the central part of the chamber which in this way is insulated from ground. This central part holds the target. A first prototype was built for experimental validation of the concept of self-biasing.

The bias potential reached a steady state value of 330 kV shortly after the rise time of the electron beam. Reduction of the X-ray spot size source of a factor 2 was thus achieved reproducibly. Finally, an improved design of bias target for standard use on AIRIX radiographic facility was built based on these results (see Fig. 3). Resistors of 420 Ω were retained. They are moulded in epoxy resin. A target is looking like a flat crown made of tantalum. It allows 20 successive shots since it can be moved in rotation from remote control. No opening of the vacuum chamber is then required allowing better statistics on spot size measurements.

Fig. 3: Open-view of the self-biased converter

More experiments to certify the concept of this self-bias target design were carried out at PIVAIR (3 kA, 5.8 MeV, 90 ns). Stabilization of the spot size using this easy to operate converter leads to a reduction of the average value over time duration .

## 5 CONCLUSION

The emission model VAPOR has been coupled to the M2V Maxwell-Vlasov PIC code to interpret the $H^+$ emission produced by the impact of the electron beam on the target of the PIVAIR facility. Simulations and experimental results are in very good agreement. The H content in Ta and Au targets measured by the thermal conductivity method is sufficient to explain the experimental results. The presence of a complete mono-layer of water at the target surface only slightly modify the results.

The comparison with other experimental results obtained on PIVAIR with C, Ti and Au targets will be continued in order to fully interpret the ionic emission effect.

## 6 ACKNOWLEDGMENTS

We wish to thank A.M. Brass from the LPCES of the CNRS UMR 8648 of the Paris-Sud University of Orsay for the analysis of hydrogen content with the H-Mat 2500 hydrogen analyser.

## 7 REFERENCES

[1] T. Kwan, "*Electron Beam-Target Interaction in the X-Ray Radiography"*, LA-UR-98-4802, LANL (1996).

[2] C. Vermare, J. Labrouche, P. Le Taillandier de Gabory, D. Villate and J. T. Donohue, "*Strong Self-Focusing of a 7.2 MeV Electron Beam Striking an Aluminized Mylar Target", IEEE Transaction on Plasma Science, Vol.27, N°6 (1999) 1566.*

[3] A. Compant La Fontaine, D. Guilhem and J.L. Lemaire, "*Measurement of the ionic emission generated by an electron-photon conversion target",* Nucl. Instr. Meth. Phys. Res. A, in press (2002).

[4] A. Compant La Fontaine, J. L. Lemaire, C. Quine and J. Segré, "*Numerical Simulations and Experimental Aspects of Space Charge Compensation in a High Energy Electron Beam",* Proceedings of EPAC 2000, Vienna, Austria (2000) 1309.

[5] Y.K. Park, P. Aghalayam and D. G. Vlachos, "*A generalized approach for predicting coverage-dependent reaction parameters of complex surface reactions: application to $H_2$ oxidation over platinum*", J. Phys. Chem. A **103** (1999) 8101.

[6] R.I. Masel, "*Principles of adsorption and reaction on solid surfaces*", John Wiley & sons, New York (1996).

[7] F. Lapique, J. Lédé, J. Villermaux, B. Cales, J.F. Baumard, A.M. Antony, G. Abdul-Aziz, D. Puechberty et M. Ledoux, "*Recherches sur la production d'hydrogene par dissociation thermique directe de la vapeur d'eau*", *Entropie, N° 11 (1983) 42.*